Bose-Einstein condensates with balanced gain and loss beyond mean-field theory

Dennis Dast,* Daniel Haag, Holger Cartarius, Jörg Main, and Günter Wunner
Institut für Theoretische Physik 1, Universität Stuttgart, 70550 Stuttgart, Germany
(Received 31 August 2016; published 1 November 2016)

Most of the work done in the field of Bose-Einstein condensates with balanced gain and loss has been performed in the mean-field approximation using the $\mathcal{PT}$-symmetric Gross-Pitaevskii equation. In this work we study the many-particle dynamics of a two-mode condensate with balanced gain and loss described by a master equation in Lindblad form whose purity periodically drops to small values but then is nearly completely restored. This effect cannot be covered by the mean-field approximation, in which a completely pure condensate is assumed. We present analytic solutions for the dynamics in the noninteracting limit and use the Bogoliubov backreaction method to discuss the influence of the on-site interaction. Our main result is that the strength of the purity revivals is almost exclusively determined by the strength of the gain and loss and is independent of the amount of particles in the system and the interaction strength. For larger particle numbers, however, strong revivals are shifted towards longer times, but by increasing the interaction strength these strong revivals again occur earlier.

DOI: 10.1103/PhysRevA.94.053601

I. INTRODUCTION

An open quantum system in which particles are injected and removed in such a way that it nevertheless supports stationary solutions is called a quantum system with balanced gain and loss. Using imaginary potentials is an elegant approach to describe the in- and outflux of particles. If the imaginary potential is $\mathcal{PT}$ symmetric [1,2] or, more generally speaking, pseudo-Hermitian [3–5] stationary solutions exist under certain conditions [6,7].

Although the concept of $\mathcal{PT}$ symmetry originates from quantum mechanics the first realization of $\mathcal{PT}$-symmetric systems succeeded in optical waveguides [8–11], and as a result the focus has somewhat shifted towards optics. However, to discuss quantum effects in systems with balanced gain and loss it is necessary to study a genuine quantum system.

A promising candidate for the realization of a genuine quantum system with balanced gain and loss is a Bose-Einstein condensate in a double-well potential with an influx of particles in one well and an outflux from the other. Such a system can be described in the mean-field limit by the Gross-Pitaevskii equation, where balanced gain and loss is introduced through a $\mathcal{PT}$-symmetric imaginary potential. This has been investigated using a double-δ potential [12] and a spatially extended double well [13], and in both cases stationary stable solutions were found. Furthermore, proposals for the realization of such a system exist by embedding the $\mathcal{PT}$-symmetric double well in a larger Hermitian system [14].

These studies were performed in the mean-field limit and thus it was assumed that all particles are in the condensed phase, i.e., the single-particle density matrix is quantum mechanically pure. However, the purity of a condensate is reduced by both the coupling to the environment and the interaction of the particles [15]. Furthermore, in systems with balanced gain and loss we are especially interested in an exchange of particles with the environment, thus, it cannot be expected that a description in the mean-field limit is appropriate. To check this expectation it is necessary to carry out an analysis in the many-particle system.

A possible many-particle description is given by a Bose-Hubbard model with $\mathcal{PT}$-symmetric complex on-site energies [16,17], however, the mean-field limit of this approach does not yield the Gross-Pitaevskii equation but only a similar equation, in which the nonlinear term is divided by the norm squared of the state. Although the normalized stationary solutions are the same as for the Gross-Pitaevskii equation the dynamics differ [18,19] and, thus, it is not the many-particle description we are looking for.

Introducing the gain and loss terms via a master equation in Lindblad form [20] where the coherent dynamics is governed by the Bose-Hubbard Hamiltonian does yield the Gross-Pitaevskii equation with imaginary potentials in the mean-field limit [21–23]. The strengths of the imaginary potentials are then given by the rate of the Lindblad superoperators. Master equations are routinely used to describe phase noise and both feeding and depleting of a Bose-Einstein condensate [15,24].

By choosing the rate of the Lindblad superoperators in an appropriate manner we obtain a quantum master equation with balanced gain and loss which has been introduced in Ref. [23]. It was shown that characteristic properties of $\mathcal{PT}$-symmetric systems such as the in-phase pulsing between the lattice sites are also supported by the master equation. Comparing the time evolution of expectation values such as the particle number showed that there is an excellent agreement between the results of the master equation with balanced gain and loss and the $\mathcal{PT}$-symmetric Gross-Pitaevskii equation.

However, the many-particle dynamics reveals that the condensate can differ substantially from a completely pure condensate as assumed in the mean-field approximation, which we could show in Ref. [25]. In fact a periodic revival of the condensate's purity is observed where the purity drops to small values but afterwards is nearly completely restored. These oscillations were found to be in phase with the oscillations of the total particle number. These results are relevant, for instance, in the context of continuous atom lasers if the pumping and outcoupling occurs at different sites [26].

Such a collapse and revival of a condensate has already been observed in an optical lattice after ramping up the potential

*dennis.dast@itp1.uni-stuttgart.de

 ©2016 American Physical Society

barrier to inhibit tunneling [27]. However, these revivals occur due to the interaction between the particles and are damped by particle losses [28,29], which stands in contrast to the purity oscillations found in systems with balanced gain and loss. In the latter case the coupling to the environment is the driver behind the revivals [25]. Also it was shown that the purity of a Bose-Einstein condensate with dissipation and phase noise can show a single revival before it decays afterwards [22,30,31].

In this paper we deepen the discussion of purity oscillations of quantum systems with balanced gain and loss by using the Bogoliubov backreaction method [32,33] in addition to directly calculating the many-particle dynamics with the master equation. The Bogoliubov backreaction method yields a closed set of differential equations for the elements of the single-particle density matrix and the covariances. Without interaction between the particles the dynamics can be solved analytically, and with interaction it is numerically much less costly. We will see that for a limited time span the Bogoliubov backreaction method is in excellent agreement with the results of the master equation and thus allows us to extend the discussion to parameter regimes that are numerically not accessible using the master equation.

The paper is ordered as follows. In Sec. II the master equation with balanced gain and loss is introduced and the Bogoliubov backreaction method is extended to systems with gain and loss. The dynamics of the noninteracting limit is solved analytically in Sec. III, which allows us to understand many effects also present with interaction. In Sec. IV the accuracy and the limitations of the Bogoliubov backreaction method are discussed by comparison with the results of the master equation. A detailed study of the purity revivals for different initial states and the influence of the initial particle number and the interaction strength follows in Sec. V. Finally, calculating the eigenvector to the macroscopic eigenvalue of the single-particle density matrix in Sec. VI allows a direct comparison with the mean-field state. Conclusions are drawn in Sec. VII.

II. TWO-MODE SYSTEM WITH BALANCED GAIN AND LOSS

The many-particle description of a Bose-Einstein condensate with balanced gain and loss introduced in Ref. [23] is given by a quantum master equation in Lindblad form. It describes a system consisting of two lattice sites with loss at site 1 and gain at site 2. The master equation is given by

$$\frac{d}{dt}\hat{\rho} = -i[\hat{H},\hat{\rho}] + \mathcal{L}_{\text{loss}}\hat{\rho} + \mathcal{L}_{\text{gain}}\hat{\rho}, \tag{1a}$$

$$\hat{H} = -J(\hat{a}_1^\dagger\hat{a}_2 + \hat{a}_2^\dagger\hat{a}_1) + \frac{U}{2}(\hat{a}_1^\dagger\hat{a}_1^\dagger\hat{a}_1\hat{a}_1 + \hat{a}_2^\dagger\hat{a}_2^\dagger\hat{a}_2\hat{a}_2), \tag{1b}$$

$$\mathcal{L}_{\text{loss}}\hat{\rho} = -\frac{\gamma_{\text{loss}}}{2}(\hat{a}_1^\dagger\hat{a}_1\hat{\rho} + \hat{\rho}\hat{a}_1^\dagger\hat{a}_1 - 2\hat{a}_1\hat{\rho}\hat{a}_1^\dagger), \tag{1c}$$

$$\mathcal{L}_{\text{gain}}\hat{\rho} = -\frac{\gamma_{\text{gain}}}{2}(\hat{a}_2\hat{a}_2^\dagger\hat{\rho} + \hat{\rho}\hat{a}_2\hat{a}_2^\dagger - 2\hat{a}_2^\dagger\hat{\rho}\hat{a}_2), \tag{1d}$$

where the bosonic creation and annihilation operators $\hat{a}_j^\dagger$ and $\hat{a}_j$ are used and we set $\hbar = 1$.

The coherent dynamics of bosonic atoms in the lowest-energy Bloch band of an optical lattice are described by the Bose-Hubbard Hamiltonian [34] in Eq. (1b). In the two-mode formulation the Hamiltonian is well suited to describe a Bose-Einstein condensate in a double-well potential [35]. The first term of Eq. (1b) describes tunneling between the two lattice sites and the second term describes an on-site interaction between the particles. The strength of the tunneling is given by the parameter J, which for all results shown in this work is taken to be $J = 1$. This choice effectively sets the time scale to $\tau = \hbar/J$. To define the strength of the on-site interaction we use the macroscopic interaction strength

$$g = (N_0 - 1)U, \tag{2}$$

which depends on the initial amount of particles N_0 in the system.

The controlled outcoupling of particles at lattice site 1 could be realized by a focused electron beam. It was demonstrated that using a commercial electron microscope it is possible to remove atoms from single sites of an optical lattice [36–38]. If an incident electron collides with an atom, the atom is ionized or excited and escapes the trapping potential. Additionally there are secondary collisions which lead to further atom losses. Since it was shown that there is almost no heating due to the electron beam it can be seen as an almost pure dissipative effect describable by a Lindblad superoperator of the form (1c).

A continuous and coherent incoupling of atoms into a Bose-Einstein condensate was experimentally realized by feeding from a second condensate [26], thus being a possible realization for the particle gain at lattice site 2. In this setup the second condensate acts as a source of particles and is located above the first condensate. By applying a continuous radio-frequency field, atoms in the source condensate make a transition from an $m_{\text{F}} = 2$ state to an $m_{\text{F}} = 0$ state. As a result they leave the magneto-optical trap and begin to fall under the action of gravity towards the lower condensate. An upward propagating light beam causes a transition of the falling atoms into a state from which they are stimulated to emit into the state of the lower condensate. A subsequent study indicated that the pumping occurs in a Raman superradiancelike process [39–41].

The parameters γ_{loss} and γ_{gain} determine the strength of the particle gain and loss. They are balanced in the following way:

$$\gamma_{\text{loss}} = \frac{N_0 + 2}{N_0}\gamma_{\text{gain}} \equiv \gamma, \tag{3}$$

which ensures that if half of the particles are at each lattice site then, for short times, the particle gain and loss have equal strength [23]. In this work we will use the abbreviation $\gamma \equiv \gamma_{\text{loss}}$ to define the strength of the in- and outcoupling and γ_{gain} is always chosen such that it fulfills Eq. (3).

The Bogoliubov backreaction method [32,33] allows us to calculate the time evolution of the single-particle density matrix instead of solving the many-particle dynamics. The time derivative of the single-particle density matrix $\sigma_{jk} = \langle\hat{a}_j^\dagger\hat{a}_k\rangle$ calculated with the master equation (1) reads

$$\frac{d}{dt}\sigma_{jk} = -iJ(\sigma_{j+1\,k} + \sigma_{j-1\,k} - \sigma_{j\,k+1} - \sigma_{j\,k-1}) - iU(\sigma_{kk}\sigma_{jk} - \sigma_{jj}\sigma_{jk} + \Delta_{jkkk} - \Delta_{jjjk})$$

$$- \frac{\gamma_{\mathrm{loss},j} + \gamma_{\mathrm{loss},k}}{2}\sigma_{jk} + \frac{\gamma_{\mathrm{gain},j} + \gamma_{\mathrm{gain},k}}{2}(\sigma_{jk} + \delta_{jk}), \tag{4}$$

where $\gamma_{\mathrm{gain},j}$ and $\gamma_{\mathrm{loss},j}$ are the strength of the gain and loss contributions at lattice site j. In this representation Eq. (4) is more general than Eqs. (1) since it holds for a Bose-Hubbard chain with arbitrary length and gain and loss at arbitrary lattice sites.

However, Eq. (4) does not yield a closed set of differential equations because of the covariances

$$\Delta_{jklm} = \langle \hat{a}_j^\dagger \hat{a}_k \hat{a}_l^\dagger \hat{a}_m \rangle - \langle \hat{a}_j^\dagger \hat{a}_k \rangle \langle \hat{a}_l^\dagger \hat{a}_m \rangle. \tag{5}$$

Neglecting the covariances, i.e. approximating second-order expectation values by a product of first-order expectation values $\langle \hat{a}_j^\dagger \hat{a}_k \hat{a}_l^\dagger \hat{a}_m \rangle \approx \langle \hat{a}_j^\dagger \hat{a}_k \rangle \langle \hat{a}_l^\dagger \hat{a}_m \rangle$, would lead to a closed set of differential equations but is only valid for large particle numbers and close to pure condensates.

The Bogoliubov backreaction improves the approximation by taking the time evolution of the covariances into account. This method has been successfully used for closed systems [32,33,42] and systems with dissipation [22], thus, we expect to obtain also accurate results for systems with both gain and loss. Calculating the time derivative of the covariances will again result in expectation values of higher order due to the nonlinear term. These third-order expectation values are approximated by a product of first-order and second-order expectation values in the following way [32]:

$$\begin{aligned}\langle \hat{a}_i^\dagger \hat{a}_j \hat{a}_k^\dagger \hat{a}_l \hat{a}_m^\dagger \hat{a}_n \rangle \approx{}& \langle \hat{a}_i^\dagger \hat{a}_j \hat{a}_k^\dagger \hat{a}_l \rangle \langle \hat{a}_m^\dagger \hat{a}_n \rangle + \langle \hat{a}_i^\dagger \hat{a}_j \hat{a}_m^\dagger \hat{a}_n \rangle \langle \hat{a}_k^\dagger \hat{a}_l \rangle \\ &+ \langle \hat{a}_k^\dagger \hat{a}_l \hat{a}_m^\dagger \hat{a}_n \rangle \langle \hat{a}_i^\dagger \hat{a}_j \rangle - 2\langle \hat{a}_i^\dagger \hat{a}_j \rangle \langle \hat{a}_k^\dagger \hat{a}_l \rangle \langle \hat{a}_m^\dagger \hat{a}_n \rangle. \end{aligned} \tag{6}$$

Using the approximation (6) the time derivatives of the covariances read

$$\begin{aligned}\frac{d}{dt}\Delta_{jklm} = {}& -iJ(\Delta_{j+1\,klm} + \Delta_{j-1\,klm} - \Delta_{j\,k+1\,lm} - \Delta_{j\,k-1\,lm} \\ &+ \Delta_{jk\,l+1\,m} + \Delta_{jk\,l-1\,m} - \Delta_{jkl\,m+1} - \Delta_{jkl\,m-1}) \\ &+ iU[\Delta_{jklm}(\sigma_{jj} - \sigma_{kk} + \sigma_{ll} - \sigma_{mm}) \\ &+ \Delta_{jjlm}\sigma_{jk} - \Delta_{kklm}\sigma_{jk} + \Delta_{jkll}\sigma_{lm} - \Delta_{jkmm}\sigma_{lm}] \\ &- \frac{\gamma_{\mathrm{loss},j} + \gamma_{\mathrm{loss},k} + \gamma_{\mathrm{loss},l} + \gamma_{\mathrm{loss},m}}{2}\Delta_{jklm} \\ &+ \delta_{kl}\gamma_{\mathrm{loss},k}\sigma_{jm} \\ &+ \frac{\gamma_{\mathrm{gain},j} + \gamma_{\mathrm{gain},k} + \gamma_{\mathrm{gain},l} + \gamma_{\mathrm{gain},m}}{2}\Delta_{jklm} \\ &+ \delta_{jm}\gamma_{\mathrm{gain},j}(\sigma_{lk} + \delta_{lk}), \end{aligned} \tag{7}$$

which form, together with Eq. (4), a closed set of differential equations.

For M lattice sites Eq. (4) yields M^2 complex equations and Eq. (7) M^4 complex equations. However, the single-particle density matrix contains only M^2 independent real elements due to $\sigma_{jk} = \sigma_{kj}^*$, and there are only $\frac{1}{2}(M^4 + M^2)$ independent real quantities for the covariances due to $\Delta_{jklm} = \Delta_{mlkj}^*$ and $\Delta_{jklm} = \Delta_{lmjk} - \delta_{jm}\sigma_{lk} + \delta_{lk}\sigma_{jm}$. When choosing the independent covariances one has to keep in mind that commutation relations for the indices of the covariances do not necessarily hold for their time derivatives given by Eq. (7) as a result of the approximation (6).

For the two-mode system considered here we can use the Bloch representation [33]. The four real independent quantities of the single-particle density matrix are then given by the expectation values $s_j = 2\langle \hat{L}_j \rangle$ and $n = \langle \hat{n} \rangle$ of the four Hermitian operators,

$$\hat{L}_x = \frac{1}{2}(\hat{a}_1^\dagger \hat{a}_2 + \hat{a}_2^\dagger \hat{a}_1), \quad \hat{L}_y = \frac{i}{2}(\hat{a}_1^\dagger \hat{a}_2 - \hat{a}_2^\dagger \hat{a}_1), \tag{8a}$$

$$\hat{L}_z = \frac{1}{2}(\hat{a}_2^\dagger \hat{a}_2 - \hat{a}_1^\dagger \hat{a}_1), \quad \hat{n} = \hat{a}_1^\dagger \hat{a}_1 + \hat{a}_2^\dagger \hat{a}_2, \tag{8b}$$

and the ten real independent covariances are the covariances between these operators

$$\Delta_{jk} = \langle \hat{A}_j \hat{A}_k + \hat{A}_k \hat{A}_j \rangle - 2\langle \hat{A}_j \rangle \langle \hat{A}_k \rangle, \tag{9}$$

where $\hat{A}_j \in \{\hat{L}_x, \hat{L}_y, \hat{L}_z, \hat{n}\}$. The time derivatives of s_j and Δ_{jk} are then given by linear combinations of Eqs. (4) and (7), respectively. They read

$$\dot{s}_x = -U(s_y s_z + 2\Delta_{yz}) - \gamma_- s_x, \tag{10a}$$

$$\dot{s}_y = 2Js_z + U(s_x s_z + 2\Delta_{xz}) - \gamma_- s_y, \tag{10b}$$

$$\dot{s}_z = -2Js_y + \gamma_+ n - \gamma_- s_z + \gamma_{\mathrm{gain}}, \tag{10c}$$

$$\dot{n} = -\gamma_- n + \gamma_+ s_z + \gamma_{\mathrm{gain}}, \tag{10d}$$

$$\begin{aligned}\dot{\Delta}_{xx} = {}& -2U(s_z\Delta_{xy} + s_y\Delta_{xz}) \\ &- \gamma_-\left(2\Delta_{xx} - \frac{s_z}{2}\right) + \gamma_+\frac{n}{2} + \frac{\gamma_{\mathrm{gain}}}{2}, \end{aligned} \tag{11a}$$

$$\begin{aligned}\dot{\Delta}_{yy} = {}& +4J\Delta_{yz} + 2U(s_z\Delta_{xy} + s_x\Delta_{yz}) \\ &- \gamma_-\left(2\Delta_{yy} - \frac{s_z}{2}\right) + \gamma_+\frac{n}{2} + \frac{\gamma_{\mathrm{gain}}}{2}, \end{aligned} \tag{11b}$$

$$\begin{aligned}\dot{\Delta}_{zz} = {}& -4J\Delta_{yz} - \gamma_-\left(2\Delta_{zz} + \frac{s_z}{2}\right) \\ &+ \gamma_+\left(\Delta_{zn} + \frac{n}{2}\right) + \frac{\gamma_{\mathrm{gain}}}{2}, \end{aligned} \tag{11c}$$

$$\begin{aligned}\dot{\Delta}_{xy} = {}& +2J\Delta_{xz} + U(s_x\Delta_{xz} + s_z\Delta_{xx} \\ &- s_z\Delta_{yy} - s_y\Delta_{yz}) - 2\gamma_-\Delta_{xy}, \end{aligned} \tag{11d}$$

$$\begin{aligned}\dot{\Delta}_{xz} = {}& -2J\Delta_{xy} - U(s_y\Delta_{zz} + s_z\Delta_{yz}) \\ &- \gamma_-\left(2\Delta_{xz} + \frac{s_x}{2}\right) + \gamma_+\frac{\Delta_{xn}}{2}, \end{aligned} \tag{11e}$$

$$\begin{aligned}\dot{\Delta}_{yz} = {}& +2J(\Delta_{zz} - \Delta_{yy}) + U(s_x\Delta_{zz} + s_z\Delta_{xz}) \\ &- \gamma_-\left(2\Delta_{yz} + \frac{s_y}{2}\right) + \gamma_+\frac{\Delta_{yn}}{2}, \end{aligned} \tag{11f}$$

$$\begin{aligned}\dot{\Delta}_{xn} = {}& -U(s_z\Delta_{yn} + s_y\Delta_{zn}) \\ &- 2\gamma_-\Delta_{xn} + \gamma_+(2\Delta_{xz} + s_x), \end{aligned} \tag{11g}$$

$$\begin{aligned}\dot{\Delta}_{yn} = {}& +2J\Delta_{zn} + U(s_x\Delta_{zn} + s_z\Delta_{xn}) \\ &- 2\gamma_-\Delta_{yn} + \gamma_+(2\Delta_{yz} + s_y), \end{aligned} \tag{11h}$$

$$\begin{aligned}\dot{\Delta}_{zn} = {}& -2J\Delta_{yn} - \gamma_-(2\Delta_{zn} + n) \\ &+ \gamma_+\left(2\Delta_{zz} + \frac{\Delta_{nn}}{2} + s_z\right) + \gamma_{\mathrm{gain}}, \end{aligned} \tag{11i}$$

$$\dot{\Delta}_{nn} = -\gamma_-(2\Delta_{nn} + 2s_z) + \gamma_+(4\Delta_{zn} + 2n) + 2\gamma_{\text{gain}}, \tag{11j}$$

with $\gamma_- = (\gamma_{\text{loss}} - \gamma_{\text{gain}})/2$ and $\gamma_+ = (\gamma_{\text{loss}} + \gamma_{\text{gain}})/2$. The differential equations of the first-order moments (10) and the second-order moments (11) are coupled via the nonlinear interaction term, i.e., terms containing the parameter U. Furthermore the differential equation of n (10d) and the covariances of n (11g)–(11j) are coupled to the remaining equations only by terms containing γ, which is not surprising since these terms arise due to the gain and loss of particles, and without them the particle number is conserved. The inhomogeneities of all differential equations contain only γ_{gain}, thus, they solely arise due to the particle gain.

Starting from Eq. (4) the mean-field approximation is obtained by assuming a pure condensate, i.e., $\sigma_{jk} = c_j^* c_k$ with the mean-field occupation coefficients c_i of site i, and neglecting the covariances. Both assumptions hold in the limit $N_0 \to \infty$. For the two-mode system with balanced gain and loss (1) the mean-field limit is the $\mathcal{PT}$-symmetric Gross-Pitaevskii equation [23],

$$i\frac{d}{dt}c_1 = -Jc_2 + g|c_1|^2 c_1 - i\frac{\gamma}{2}c_1, \tag{12a}$$

$$i\frac{d}{dt}c_2 = -Jc_1 + g|c_2|^2 c_2 + i\frac{\gamma}{2}c_2. \tag{12b}$$

In the mean-field limit a state is defined by two complex numbers $c = (c_1,\ c_2)^T$, whereas only two real degrees of freedom remain due to normalization and the choice of a global phase. The corresponding many-particle state with a total number of N_0 particles is, in the Fock basis $|n_1,n_2\rangle$, given by [23]

$$|\psi\rangle = \sum_{m=0}^{N_0} \sqrt{\binom{N_0}{m}} c_1^{N_0-m} c_2^m |N_0 - m, m\rangle. \tag{13}$$

The Gross-Pitaevskii equation (12) supports two $\mathcal{PT}$-symmetric stationary solutions

$$c_1 = \pm\frac{1}{\sqrt{2}} \exp\left[\pm i \operatorname{asin}\left(\frac{\gamma}{2J}\right)\right], \quad c_2 = \frac{1}{\sqrt{2}}, \tag{14}$$

which exist for $|\gamma| \leqslant 2J$ and which we will call the ground (positive signs) and excited state (negative signs) of the system [17,23]. In addition there are two $\mathcal{PT}$-broken solutions for $|\gamma| \geqslant \sqrt{4J^2 - g^2}$.

In this work we use results obtained by directly solving the master equation (1) via the quantum jump method [43,44] and results obtained by integrating the differential equations (10) and (11) of the Bogoliubov backreaction method. For the quantum jump method an average over a certain amount of quantum trajectories is performed till the results converge.

The essential quantity discussed in this work is the purity of the reduced single-particle density matrix $\sigma_{\text{red},jk} = \sigma_{jk}/\operatorname{tr}\sigma$, which measures how close the condensate is to a pure Bose-Einstein condensate,

$$P = 2\operatorname{tr}\sigma_{\text{red}}^2 - 1 = \frac{s_x^2 + s_y^2 + s_z^2}{n^2} \in [0,1]. \tag{15}$$

A pure condensate with $P = 1$ is described by a product state as it is assumed for the Gross-Pitaevskii equation. In this case all particles are in the condensed mode since all but one eigenvalue of σ_{red} vanish. An increasing occupation of the noncondensed mode reduces the value of P. If more than one eigenvalue is large the condensate is called fragmented [45].

For a given initial particle number N_0 a pure state has only two degrees of freedom,

$$s_x = N_0 \sin(\vartheta)\cos(\varphi), \tag{16a}$$

$$s_y = N_0 \sin(\vartheta)\sin(\varphi), \tag{16b}$$

$$s_z = N_0 \cos(\vartheta). \tag{16c}$$

In the following pure states will therefore be characterized by the two angles φ and ϑ. They are obtained from the normalized $c_{1/2}$ by $\vartheta = \operatorname{acos}(1 - 2|c_1|^2)$ and $\varphi = \arg(c_1 c_2^*)$. Accordingly the two $\mathcal{PT}$-symmetric solutions (14) are given by $\vartheta = \pi/2$ and $\varphi = \pi/2 \mp \operatorname{acos}(\gamma/2J)$.

The purity of the condensate can be measured in interference experiments where the double-well trap is turned off and as a result the condensate expands and interferes [46,47]. The average contrast [30,31,46] in such an experiment is obtained by averaging over various realizations [48] and is given by

$$v = \frac{2|\langle \hat{a}_1^\dagger \hat{a}_2\rangle|}{\langle \hat{a}_1^\dagger \hat{a}_1\rangle + \langle \hat{a}_2^\dagger \hat{a}_2\rangle} = \frac{\sqrt{s_x^2 + s_y^2}}{n} \in [0,1]. \tag{17}$$

By introducing the squared imbalance of the particle number in the two lattice sites

$$I = \left(\frac{\langle \hat{a}_1^\dagger \hat{a}_1\rangle - \langle \hat{a}_2^\dagger \hat{a}_2\rangle}{\langle \hat{a}_1^\dagger \hat{a}_1\rangle + \langle \hat{a}_2^\dagger \hat{a}_2\rangle}\right)^2 = \frac{s_z^2}{n^2} \in [0,1], \tag{18}$$

the squared average contrast can be written as

$$v^2 = P - I. \tag{19}$$

This shows that the purity is the upper limit for the squared contrast and for equally distributed particles the two quantities are identical.

III. NONINTERACTING LIMIT

For vanishing interaction, i.e., $U = 0$, the differential equations of the first-order moments (10) and the second-order moments (11) decouple. Thus, the first-order moments already yield a closed set of linear differential equations

$$\dot{s}_x = -\gamma_- s_x, \tag{20a}$$

$$\dot{s}_y = 2Js_z - \gamma_- s_y, \tag{20b}$$

$$\dot{s}_z = -2Js_y + \gamma_+ n - \gamma_- s_z + \gamma_{\text{gain}}, \tag{20c}$$

$$\dot{n} = -\gamma_- n + \gamma_+ s_z + \gamma_{\text{gain}}, \tag{20d}$$

which can be solved analytically.

There is an oscillatory regime for $4J^2 > \gamma_+^2$ in which the solution reads

$$s_x(t) = \kappa_1 e^{-\gamma_- t}, \tag{21a}$$

$$s_y(t) = \alpha_2 + [\gamma_+\kappa_2 + 2J\kappa_3\cos(\omega t - \kappa_4)]e^{-\gamma_- t}, \tag{21b}$$

$$s_z(t) = \alpha_3 - \omega\kappa_3 \sin(\omega t - \kappa_4)e^{-\gamma_- t}, \quad (21c)$$

$$n(t) = \alpha_4 + [2J\kappa_2 + \gamma_+\kappa_3 \cos(\omega t - \kappa_4)]e^{-\gamma_- t}, \quad (21d)$$

with $\omega = \sqrt{4J^2 - \gamma_+^2}$, the steady state of the system

$$\boldsymbol{\alpha} = \frac{\gamma_+^2 - \gamma_-^2}{4J^2 - \gamma_+^2 + \gamma_-^2} \begin{pmatrix} 0 \\ \frac{2J}{\gamma_-} \\ 1 \\ 1 + \frac{4J^2}{\gamma_-(\gamma_+ + \gamma_-)} \end{pmatrix}, \quad (22)$$

and the four real parameters κ_i that define the initial state.

As can be directly seen the steady state is an attractor and every trajectory will finally reach this state with the decay rate γ_-. For balanced gain and loss as defined in Eq. (3) the decay rate is given by $\gamma_- = \gamma_{\text{gain}}/N_0$.

The short-term behavior is dominated by oscillations with the characteristic frequency ω. The frequency is maximum for vanishing gain and loss, $\gamma_+ \to 0$, and decreases to zero for $\gamma_+ \to 2J$.

Since the purity oscillations discussed in Ref. [25] are driven by the gain and loss of the system and not by the interaction of the particles the purity oscillations are also present in the noninteracting limit, thus giving us access to an analytic discussion of the properties of the purity.

The dynamical behavior of the purity consists of fast oscillations with frequency ω, which are confined by an envelope function as shown in Figs. 1(b) and 1(c).

The lower and upper envelope functions are very precisely given by

$$P_{\text{l/u}} = \frac{\kappa_1^2 + (\alpha_2 e^{\gamma_- t} + \gamma_+\kappa_2 \mp 2J|\kappa_3|)^2 + \alpha_3^2 e^{2\gamma_- t}}{(\alpha_4 e^{\gamma_- t} + 2J\kappa_2 \mp \gamma_+|\kappa_3|)^2}. \quad (23)$$

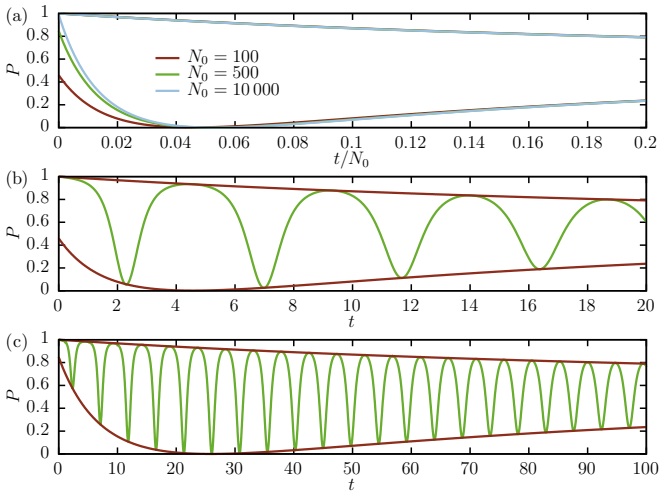

FIG. 1. (a) The envelope functions of the purity oscillations (23) for three different initial particle numbers in the noninteracting limit. The time is scaled by the particle number in such a way that the envelope functions become similar for large particle numbers. Although the particle number changes the time scale of the envelope the period of the actual oscillations stays approximately the same as can be seen for (b) $N_0 = 100$ and (c) $N_0 = 500$. In all calculations the pure initial state $\varphi = \vartheta = \pi/2$ and the gain-loss parameter $\gamma = 1.5$ were used.

These envelope functions are obtained by calculating the purity (15) for the solutions (21) and setting $\kappa_3 \cos(\omega t - \kappa_4) = \mp|\kappa_3|$ and $\kappa_3 \sin(\omega t - \kappa_4) = 0$.

Since the initial particle number N_0 is much larger than the system parameters J and γ, and the initial values for $s_{x,y,z}$ all scale with N_0, we can expand Eq. (23) in powers of N_0. This is done for all terms except the time dependent term $e^{\gamma_- t}$ since t might be large. The calculation shows that the leading order of both the numerator and the denominator is N_0^2. By neglecting all other orders the remaining influence of N_0 is only in the exponential term $e^{\gamma_- t}$. With Eq. (3) we can write $\gamma_- = \gamma_{\text{loss}}/(N_0 + 2) \approx \gamma_{\text{loss}}/N_0$ and thus $e^{\gamma_- t} \approx e^{\gamma_{\text{loss}} t/N_0}$.

This shows that for $N_0 \gg 1$ the initial particle number only changes the time scale of $P_{\text{l/u}}$. Multiplying N_0 with a factor effectively stretches the time scale by this factor. Thus, the dynamics of the envelope functions are slower for higher particle numbers. Since the envelope functions define the strength of the purity revivals we can conclude that not the strength of the revivals is changed by N_0 but only the time at which strong revivals occur.

This can be checked in Fig. 1(a), which shows the envelope functions for three different initial particle numbers N_0. The rescaled time parameter t/N_0 is used so that we expect all envelopes to become similar for $N_0 \gg 1$. In fact the upper envelope function is virtually identical for all particle numbers. The lower envelope function is different in the initial area and especially $P_{\text{l}}(t = 0)$ has different values. This difference, however, vanishes for large particle numbers and consequently the difference between $N_0 = 10\,000$ and $N_0 = 500$ is much smaller than that between $N_0 = 500$ and $N_0 = 100$. For $t/N_0 \gtrsim 0.04$ also the lower envelope functions lie almost perfectly on top of each other.

Note that the frequency of the fast oscillations with $\omega = \sqrt{4J^2 - \gamma_+^2}$ is mostly unaffected by N_0 since $\gamma_+ = \gamma_{\text{loss}}(N_0 + 1)/(N_0 + 2) \approx \gamma_{\text{loss}}$. This explains the behavior shown in Figs. 1(b) and 1(c), which compares the purity oscillations for $N_0 = 100$ and $N_0 = 500$. The oscillation frequency is approximately the same but the time scale of the envelope functions in Fig. 1(c) is stretched by a factor of 5. As a result the first purity revivals for $N_0 = 500$ are small and they become only stronger once the difference of the envelope functions becomes larger, whereas for $N_0 = 100$ already the first purity revival is strong.

IV. ACCURACY OF THE BOGOLIUBOV BACKREACTION METHOD

With interaction between the particles the differential equations of first order couple to the second-order moments and we can no longer solve this set of nonlinear differential equations analytically. Instead Eqs. (10) and (11) are integrated numerically. It is not *a priori* clear that the Bogoliubov backreaction method yields precise results for this system since the expansion in higher order expectation values converges in powers of the smaller eigenvalue of σ_{red} [32,33]. Thus we can only be sure to obtain accurate results as long as the condensate remains almost pure, i.e., the matrix σ_{red} has one eigenvalue close to one and the remaining eigenvalue is close to zero.

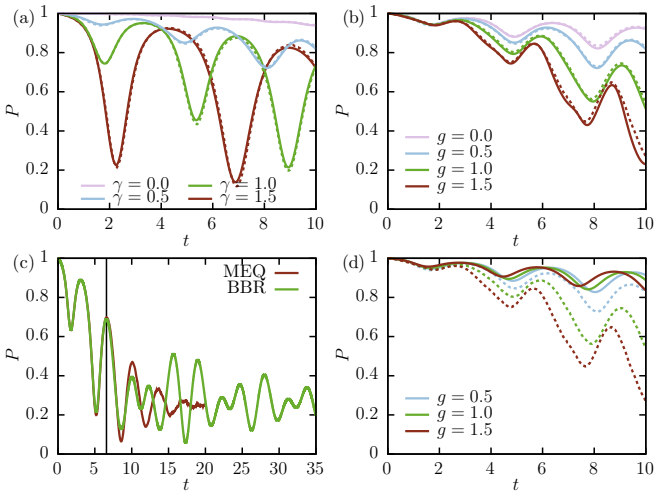

FIG. 2. Time evolution of the purity P for different values of (a) the gain-loss parameter γ (with $g = 0.5$) and (b) the interaction strength g (with $\gamma = 0.5$). The results obtained with the Bogoliubov backreaction method (solid lines) are in excellent agreement with the results obtained with the many-particle calculations (dotted lines) but for stronger interaction the agreement is slightly worse. In these calculations the pure initial state $\varphi = \vartheta = \pi/2$ and the particle number $N_0 = 100$ were used. For the master equation it was averaged over 500 trajectories. For longer times (c) the Bogoliubov backreaction method (BBR) shows a behavior similar to a beat frequency that is not observed using the master equation (MEQ). This is used to define the last maximum of the purity where the revival strength still increases as the limit for the reliability of the Bogoliubov backreaction method (marked by the black vertical line). The parameters used are $\varphi = \vartheta = \pi/2, \gamma = 1, g = 1, N_0 = 50$ and for the master equation it was averaged over 3000 trajectories. (d) Neglecting the covariances in Eq. (4) (solid lines) shows a behavior that differs substantially from the many-particle calculations (dotted lines). The parameters used are $\gamma = 0.5$ and $N_0 = 100$.

To evaluate the accuracy of the Bogoliubov backreaction method it is compared with results directly obtained using the master equation (1). Figure 2(a) compares the results of the two approaches for different values of the gain-loss parameter with constant interaction strength $g = 0.5$. The results obtained with the Bogoliubov backreaction method (dotted lines) lie nearly perfectly on top of the results obtained with the master equation (solid lines) for all trajectories shown. Comparing all elements of the single-particle density matrix and the covariances confirms this excellent agreement. It is especially remarkable that even for $\gamma = 1.5$ where the purity of the condensate drops to very small values, thus, violating the aforementioned condition, the numerical results nevertheless show this excellent agreement.

Since the approximation of the Bogoliubov backreaction method is applied to the nonlinear interaction term it is expected that the approximation becomes worse for stronger interactions. Figure 2(b) shows the time evolution of the purity for different values of g but with an identical gain-loss parameter $\gamma = 0.5$ and compares the results of the master equation with those of the Bogoliubov backreaction method. Note that there is even a small discrepancy for $g = 0$ where the dynamics of the single-particle density matrix (10) is exact. This discrepancy stems from the fact that the quantum jump method is not exact itself but only becomes exact in the limit of infinitely many quantum trajectories. As expected for stronger nonlinearities the discrepancy between the two different approaches becomes slightly larger but is still very good.

There is, however, a fundamental difference between the results of the two approaches for longer times as illustrated by a sample trajectory in Fig. 2(c). After a few purity oscillations the Bogoliubov backreaction method shows a behavior similar to a beat frequency where the amplitude of the oscillations increases and decreases periodically. This behavior is not found using the many-particle calculations at all. We can now use this observation to identify a limit for the reliability of the Bogoliubov backreaction method. For all trajectories checked we found that the purity revival from one minimum to the subsequent maximum increases for the first oscillations, i.e. $\Delta P_i = P_{\max,i} - P_{\min,i}$ increases with i. It decreases for the first time when the first node of the beat frequency is approached. Thus, we use the last maximum where the revival strength still increases as the limit for the Bogoliubov backreaction method. This limit is visualized in Fig. 2(c) by the vertical black line.

Since within this limit there is an excellent agreement between the Bogoliubov backreaction method and the many-particle dynamics one might ask if it is even necessary to take the covariances into account. As mentioned in Sec. II a closed set of equations for the single-particle density matrix is also obtained if we neglect the covariances in Eq. (10), which is equivalent to the approximation $\langle \hat{a}_j^\dagger \hat{a}_k \hat{a}_l^\dagger \hat{a}_m \rangle \approx \langle \hat{a}_j^\dagger \hat{a}_k \rangle \langle \hat{a}_l^\dagger \hat{a}_m \rangle$.

The results obtained in this approximation are shown in Fig. 2(d) (solid lines) compared with the many-particle dynamics (dotted lines) for different values of the macroscopic interaction g. Using this approximation we still find oscillations of the purity and also the frequency of the oscillation, which increases for larger values of g, is well captured. However, the actual values of the purity differ substantially. The many-particle calculations show considerably smaller purities, and the purities become smaller for increasing values of g. If the covariances are neglected this influence of the interaction is not found. Instead the purity stays even closer to unity for stronger interactions.

This shows that to understand the physics of a system with balanced gain and loss it is necessary to take the covariances into account. The covariances are fluctuations that are driven by the single-particle density matrix but they also yield a backreaction by the coupling terms proportional to U. These fluctuations alter the behavior of the system in an essential manner and are the leading corrections to the dynamics since it is not necessary to consider higher orders to obtain accurate results.

V. PURITY REVIVALS

In this section we perform a detailed analysis of the purity revivals using the Bogoliubov backreaction method. Our main interest is to study how the revivals depend on the gain-loss parameter γ and the interaction strength g. To characterize the strength of the purity oscillations we use the strongest purity revival ΔP, i.e., the greatest increase from a purity minimum to the subsequent maximum. As discussed in the previous

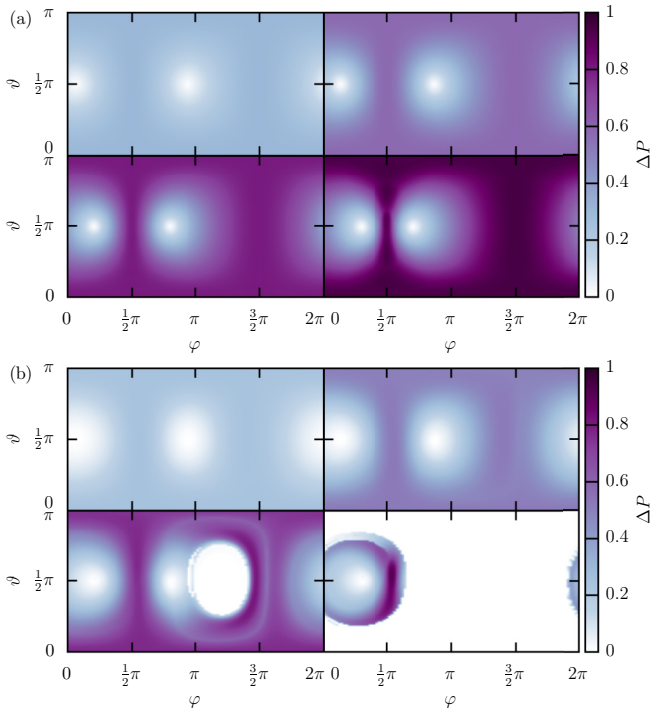

FIG. 3. The strongest purity revivals ΔP for pure initial states defined by the two parameters φ and ϑ for (a) $g = 0$ and (b) $g = 0.5$. The gain-loss parameters for both (a) and (b) are $\gamma = 0.4$ (upper left), $\gamma = 0.8$ (upper right), $\gamma = 1.2$ (lower left), and $\gamma = 1.6$ (lower right). There are two distinct areas in (a) where the strength of the revivals is reduced. In the center of these areas lie the stationary ground (left area) and excited (right area) states (14) of the $\mathcal{PT}$-symmetric Gross-Pitaevskii equation. With interaction (b) an additional region with $\Delta P = 0$ arises for stronger values of γ (lower panels). This is the unstable region, in which the particle number diverges and, thus, no stable revivals occur. For increasing values of γ this region expands and for $\gamma = 1.6$ only a small area of initial states with stable revivals survives.

section the Bogoliubov backreaction method yields accurate results till the revival strength decreases, so the last purity revival that is within reach of the Bogoliubov backreaction method can be taken as the strongest revival. This strongest revival, however, does not only depend on the parameters of the system but also on the choice of the initial state. Since the initial state is always pure, it is defined by the two parameters φ and ϑ for a given particle number [see Eq. (16)].

To get an impression of the purity strength for different initial states the strongest revival is calculated as a function of φ and ϑ. Since the Bogoliubov backreaction method requires only little numerical effort we can do this for many initial values. In this case we use 100 values for both φ and ϑ, thus, in total 10 000 different initial states for each parameter set γ and g. Such a calculation would be out of reach using the quantum jump method to directly calculate the many-particle dynamics of the master equation.

Figure 3(a) shows the strongest revival in the noninteraction limit $g = 0$ for four different values of γ which all show a similar structure. For most initial states a similar strength of the revivals is found. As γ is increased so is the strength of the revivals. In the lower right panel the gain-loss parameter is $\gamma = 1.6$ and it can be seen that most initial states even lead to revivals which are close to one. In these cases the purity is completely destroyed but then is nearly fully restored. Furthermore, all four panels show two distinct areas where the strength of the revivals drops to zero. In the center of these two areas lie the two stationary $\mathcal{PT}$-symmetric states of the Gross-Pitaevskii equation (14). The left area can be identified with the ground state of the system and the right area with the excited state. As discussed in Ref. [25] these states do not show purity oscillations but instead the purity decays continuously which explains why the strength of the revivals vanishes. In the vicinity of the two stationary states the purity oscillations are less pronounced and thus the strength of the revivals is also reduced for nearby states. It can also be seen that the two areas with weak revivals approach each other as γ is increased. This is a result of the fact that the two $\mathcal{PT}$-symmetric states coalesce in an exceptional point at $\gamma = 2J$ (here $J = 1$). For $\gamma = 2J$ both the ground and excited state are then given by $c_1 = i/\sqrt{2}$ and $c_2 = 1/\sqrt{2}$ or equivalently $\varphi = \vartheta = \pi/2$.

The influence of the particle interaction on the purity revivals is shown in Fig. 3(b). For small values of the gain-loss parameter γ (upper two panels) the behavior is similar to the noninteraction limit with the difference that the areas with weak revivals are larger. In the lower left panel a new type of area arises on the right-hand side of the excited state where no revivals occur. This is the unstable region where the particle number diverges due to the particle gain. One has to be careful when analyzing the revivals in this region since a diverging state approaches a pure condensate. This happens since nearly all particles are in the lattice site with gain which implies $s_z \approx n$ and thus $P \approx 1$. However, we are only interested in stable revivals and consequently these unstable revivals are excluded. For increasing values of the gain-loss parameter γ the unstable region grows and for $\gamma = 1.6$ in the lower right panel only a small region of stable revivals survives in the vicinity of the ground state. In this parameter region strong oscillations are only found at $\varphi \approx \pi/2$.

The observation that an unstable region arises close to the excited state which expands for increasing strength of the gain and loss and finally only a small stable region near the ground state survives is also found for the $\mathcal{PT}$-symmetric Gross-Pitaevskii equation and was discussed in detail for a spatially extended double-well potential in Ref. [19]. Note that in this reference an attractive interaction was used in contrast to the repulsive interaction used in this work, which essentially switches the roles of the ground and excited state for the stability discussion.

While showing the purity revivals for different initial values gives an excellent overview, it is less suitable to quantitatively discuss the revival strength for different parameter values. To do so we search the initial state that, for constant values of the parameters g, γ, and N_0, leads to the strongest revival, i.e., the maximum in one of the panels of Fig. 3. This is implemented using a root search which varies φ and ϑ such that

$$\frac{\partial \Delta P}{\partial \varphi} = \frac{\partial \Delta P}{\partial \vartheta} = 0 \tag{24}$$

is fulfilled. Note that ΔP denotes the maximum revival reached from a specific initial state which was used in Fig. 3 to

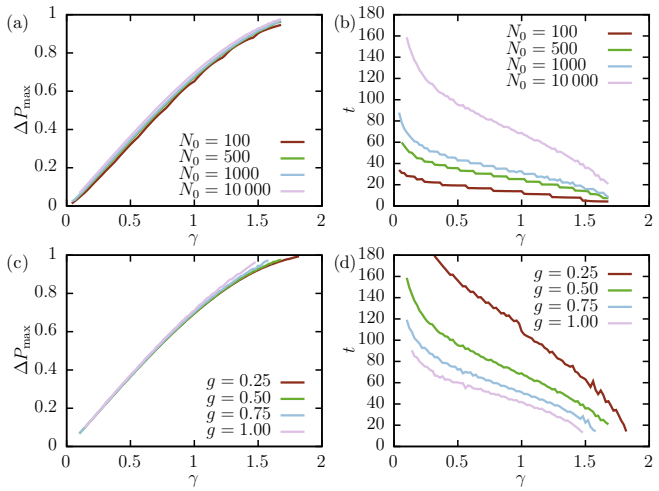

FIG. 4. (a) The parameter $\Delta P_{\max}$ is obtained by searching for the initial state that leads to the strongest purity revival ΔP. The value of $\Delta P_{\max}$ is shown as a function of the gain-loss parameter γ for four different values of the initial particle number N_0 and constant interaction strength $g = 0.5$. The revival strength increases with γ but hardly depends on N_0. (b) The times at which the revivals shown in (a) occur. For larger initial particle numbers the strongest revivals occur at later times, however, the difference is much smaller compared to the noninteracting limit where the time scales linearly with the particle number. (c) Same as (a) but for a constant large particle number $N_0 = 10\,000$ and different values of the interaction strength g. The revival strength is mostly unaffected by the value of g. (d) The times at which the revivals shown in (c) occur. For stronger interaction the maximum revivals occur at smaller times.

characterize the revival strength. Now we search for the initial state where ΔP is maximum and name this quantity $\Delta P_{\max}$.

The maximum value of ΔP as a function of the gain-loss parameter γ is shown for different initial particle numbers and constant interaction strength $g = 0.5$ in Fig. 4(a). Since the revivals are driven by the gain and loss of the system, the strength of the revivals increases with the gain-loss parameter γ. For $\gamma \to 0$ the revivals vanish and for strong gain and loss, $\Delta P_{\max}$ is close to one. However, the remarkable property is that the particle number N_0 has almost no influence on $\Delta P_{\max}$. This seems counterintuitive at first glance since for $N_0 \to \infty$ the system can be described by the $\mathcal{PT}$-symmetric Gross-Pitaevskii equation where the condensate is completely pure and, thus, no purity revivals occur. However, from the behavior in the noninteracting limit discussed in Sec. III we know that different initial particle numbers change the time scale of the envelope functions of the purity oscillations. Consequently, in this limit the strength of the strongest revival is approximately the same for different initial particle numbers but only the time at which these revivals occur changes.

Indeed we also find that with interaction the maximum revivals occur at later times. This is shown in Fig. 4(b) where the times are shown at which the maximum revivals $\Delta P_{\max}$ of Fig. 4(a) occur. There is, however, a crucial difference in the scaling behavior of the time. In the noninteracting limit the time scales linearly with the particle number and as a result the maximum revivals of $N_0 = 10\,000$ occur at times that are larger by a factor of 100 compared to the revivals of $N_0 = 100$. With interaction the difference is much smaller and we find a factor that is smaller than 10.

To investigate the influence of the interaction on the purity revivals in more detail, $\Delta P_{\max}$ is calculated for different values of the interaction strength g for a constant large particle number $N_0 = 10\,000$. Figure 4(c) shows that again the actual value of the maximum purity revivals is mostly unaffected by the interaction strength. Since neither the particle number N_0 nor the interaction strength g has a significant impact on $\Delta P_{\max}$, we can conclude that the strength of the maximum revivals is almost entirely determined by the gain-loss parameter γ.

The interaction between the particles, however, also has an impact on the times at which the strongest revivals occur as can be seen in Fig 4(d). We find that for stronger interactions the maximum revivals occur at shorter times. This is an important result since the lifetime of a Bose-Einstein condensate in an experiment is limited and without the on-site interaction significant purity oscillations only occur at very large times for a realistic number of particles. However, our results show that by adjusting the interaction strength it is possible to shift these strong purity oscillations towards shorter times.

VI. EIGENVECTORS OF THE SINGLE-PARTICLE DENSITY MATRIX

In this section we study the behavior of the condensed mode. This can be discussed using the eigenvalues and eigenvectors of the transposed reduced single-particle density matrix. The two eigenvalues give the fraction of particles in the condensed and the noncondensed phase. For the two-mode system considered here the eigenvalues contain the same information as the purity and can be written as $\lambda_{1/2} = \frac{1}{2}(1 \pm \sqrt{P})$. Thus, the eigenvalues show a similar behavior as the purity which can be seen in Fig. 5(a) for the stationary ground state and two oscillating states at different values of the gain-loss parameter.

Since the eigenvector to the macroscopic eigenvalue is the single-particle state of the condensed phase [49] it is possible to directly compare this eigenvector with the mean-field state of the Gross-Pitaevskii equation. This extends the discussion in Ref. [23], in which expectation values of the master equation and the $\mathcal{PT}$-symmetric Gross-Pitaevskii equation were compared.

We will check whether the condensed mode of the many-particle description behaves stationary if we use the stationary states of the $\mathcal{PT}$-symmetric Gross-Pitaevskii equation as initial states. For the ground state this comparison is shown in Fig. 5(b) and a similar result can of course be obtained for the excited state. The comparison shows that indeed also the state itself stays constant. Note that the underlying density matrix entering the master equation is not stationary at all but its purity rapidly decays. Nevertheless the single-particle density matrix stays approximately pure and the eigenvector to the macroscopic eigenvalue behaves stationary.

Figures 5(c) and 5(d) show the same comparison for an oscillating state for $\gamma = 1$ and $\gamma = 1.5$, respectively. In the case $\gamma = 1$ the normalized expectation values of the particle number in the jth lattice sites $|c_j| = \langle n_j \rangle / N_0$ of the many-particle calculations (solid lines) is in very good agreement with the mean-field calculations (dotted lines). The relative phase $\arg(c_1 c_2^*)$, however, shows significant deviations

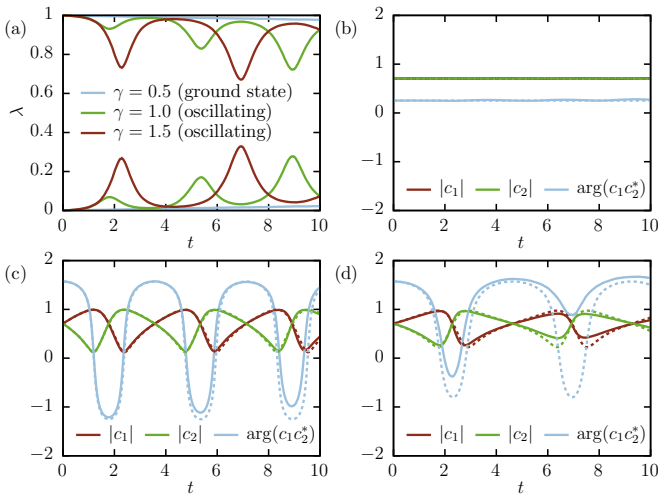

FIG. 5. (a) The two eigenvalues of the transposed reduced single-particle density matrix using the ground state of the $\mathcal{PT}$-symmetric Gross-Pitaevskii equation and the oscillating state $\varphi = \vartheta = \pi/2$ for different values of the gain-loss parameter γ as initial states. The expectation values of the particle number in the two lattice sites $|c_j| = \langle n_j \rangle / N_0$ and the relative phase $\arg(c_1 c_2^*)$ of the eigenvector to the greater eigenvalue are shown for (b) the ground state at $\gamma = 0.5$ and for the oscillating state at (c) $\gamma = 1.0$ and (d) $\gamma = 1.5$. The results of the master equation (solid lines) are compared with those of the Gross-Pitaevskii equation (dotted lines). They show that the eigenvector of the ground state behaves indeed stationary when using the master equation (note that $|c_1| \approx |c_2|$). For the oscillating state the many-particle calculations deviate from the mean-field calculations at times where the purity has a dip, and is in good agreement at times where the purity is restored. In all calculations the parameters $g = 0.5$ and $N_0 = 100$ were used and it was averaged over 500 trajectories.

at precisely the times where the purity of the single-particle density matrix has a dip. Consequently the relative phase agrees with the mean-field limit at times where the purity is restored. For $\gamma = 1.5$ an equivalent behavior is found but the discrepancy to the mean-field limit is greater especially for the relative phase.

VII. CONCLUSION

We have studied a Bose-Einstein condensate with balanced gain and loss described by a quantum master equation whose mean-field limit is a $\mathcal{PT}$-symmetric Gross-Pitaevskii equation. It is already known that the condensate's purity undergoes strong periodic revivals [25], an effect that cannot be captured using the mean-field limit where a product state, i.e., a pure condensate, is assumed. These revivals have a direct impact on the contrast measured in interference experiments. In this work we deepened the discussion of the purity oscillations by presenting an analytical solvable model for the noninteracting limit and by studying the interplay between the interaction strength and the gain and loss of particles.

To do so we applied the Bogoliubov backreaction method to systems with gain and loss. In the noninteracting limit this yields an analytically solvable model for the elements of the single-particle density matrix. Since the purity oscillations are driven by the gain and loss of the system these characteristic oscillations are also found in this limit. We showed that the frequency of the purity oscillations is mostly unaffected by the initial amount of particles in the system. However, the time scale of the envelope functions of the purity has a linear dependency on the initial particle number. As a result the time at which strong purity revivals are found is proportional to the particle number and, thus, is very large for realistic condensates.

With interaction the dynamics described by the Bogoliubov backreaction method is an approximation and its accuracy has to be checked. This has been done by a comparison with many-particle calculations using the master equation and the quantum jump method. Motivated by this comparison we formulated a limit for the reliability of the Bogoliubov backreaction method. Within this limit an excellent agreement between the two approaches was found.

Since the Bogoliubov backreaction method takes into account the backreaction of the covariances on the single-particle density matrix, it allows us to quantify the importance of the covariances. Neglecting this backreaction yields results that differ substantially compared with the many-particle dynamics. Thus we can conclude that these covariances are essential to understand the physics of systems with balanced gain and loss.

The main benefit of the Bogoliubov backreaction method is that it requires only little numerical effort. Thus, we were able to characterize the strength of the purity revivals for all possible initial pure states. This showed that apart from an area in the vicinity of the $\mathcal{PT}$-symmetric stationary states of the Gross-Pitaevskii equation strong revivals are found independent of the initial state. For stronger gain and loss there is, however, an increasing unstable area where no stable revivals can be found, and for strong gain-loss contributions only the area around the $\mathcal{PT}$-symmetric ground state of the mean-field limit is stable.

Since for the Bogoliubov backreaction method the particle number is only a parameter that does not change the numerical costs, it is easy to extend the discussion to larger particle numbers that would not be accessible using the master equation. The calculations showed that both the particle number and the strength of the on-site interaction have little impact on the actual revival strength which consequently is almost exclusively determined by the strength of the gain and loss contributions. As in the noninteracting limit, the times at which the strong revivals occur increases for larger particle numbers, but with interaction the influence is considerably smaller. Increasing the interaction strength even shifts the strong purity oscillations towards earlier times. This is an important effect for the experimental observability of the purity oscillations in systems with balanced gain and loss since the lifetime of a condensate in an experiment is limited.

Finally the single-particle state of the condensed phase, i.e., the state corresponding to the macroscopic eigenvalue of the single-particle density matrix was compared with the mean-field state that enters the Gross-Pitaevskii equation. We found a very good agreement between these states at times where the purity is high, whereas there is a significant discrepancy, especially for the relative phase, if the purity has a dip. For the stationary states of the Gross-Pitaevskii equation

the single-particle state of the condensed phase showed a stationary behavior since the single-particle density matrix is approximately stationary although the underlying density matrix entering the master equation is not.

As a next step we will study the steady state of the system. In the noninteracting limit the steady state is an attractor and its form was given in this work, but it will be interesting to also investigate its behavior for interacting particles.

[1] C. M. Bender and S. Boettcher, Phys. Rev. Lett. **80**, 5243 (1998).
[2] C. M. Bender, S. Boettcher, and P. N. Meisinger, J. Math. Phys. **40**, 2201 (1999).
[3] A. Mostafazadeh, J. Math. Phys. **43**, 205 (2002).
[4] A. Mostafazadeh, J. Math. Phys. **43**, 2814 (2002).
[5] A. Mostafazadeh, J. Math. Phys. **43**, 3944 (2002).
[6] F. M. Fernández, R. Guardiola, J. Ros, and M. Znojil, J. Phys. A **31**, 10105 (1998).
[7] F. M. Fernández and J. Garcia, J. Math. Phys. **55**, 042107 (2014).
[8] S. Klaiman, U. Günther, and N. Moiseyev, Phys. Rev. Lett. **101**, 080402 (2008).
[9] C. E. Rüter, K. G. Makris, R. El-Ganainy, D. N. Christodoulides, M. Segev, and D. Kip, Nat. Phys. **6**, 192 (2010).
[10] A. Guo, G. J. Salamo, D. Duchesne, R. Morandotti, M. Volatier-Ravat, V. Aimez, G. A. Siviloglou, and D. N. Christodoulides, Phys. Rev. Lett. **103**, 093902 (2009).
[11] B. Peng, Ş. K. Özdemir, F. Lei, F. Monifi, M. Gianfreda, G. L. Long, S. Fan, F. Nori, C. M. Bender, and L. Yang, Nat. Phys. **10**, 394 (2014).
[12] H. Cartarius and G. Wunner, Phys. Rev. A **86**, 013612 (2012).
[13] D. Dast, D. Haag, H. Cartarius, G. Wunner, R. Eichler, and J. Main, Fortschr. Phys. **61**, 124 (2013).
[14] M. Kreibich, J. Main, H. Cartarius, and G. Wunner, Phys. Rev. A **87**, 051601(R) (2013).
[15] J. Ruostekoski and D. F. Walls, Phys. Rev. A **58**, R50 (1998).
[16] E. M. Graefe, U. Günther, H. J. Korsch, and A. E. Niederle, J. Phys. A **41**, 255206 (2008).
[17] E.-M. Graefe, J. Phys. A **45**, 444015 (2012).
[18] D. Dast, D. Haag, H. Cartarius, J. Main, and G. Wunner, J. Phys. A **46**, 375301 (2013).
[19] D. Haag, D. Dast, A. Löhle, H. Cartarius, J. Main, and G. Wunner, Phys. Rev. A **89**, 023601 (2014).
[20] H.-P. Breuer and F. Petruccione, *The Theory of Open Quantum Systems*, 1st ed. (Oxford University Press, Oxford, 2002).
[21] F. Trimborn, D. Witthaut, and S. Wimberger, J. Phys. B **41**, 171001 (2008).
[22] D. Witthaut, F. Trimborn, H. Hennig, G. Kordas, T. Geisel, and S. Wimberger, Phys. Rev. A **83**, 063608 (2011).
[23] D. Dast, D. Haag, H. Cartarius, and G. Wunner, Phys. Rev. A **90**, 052120 (2014).
[24] J. Anglin, Phys. Rev. Lett. **79**, 6 (1997).
[25] D. Dast, D. Haag, H. Cartarius, and G. Wunner, Phys. Rev. A **93**, 033617 (2016).
[26] N. P. Robins, C. Figl, M. Jeppesen, G. R. Dennis, and J. D. Close, Nat. Phys. **4**, 731 (2008).
[27] M. Greiner, O. Mandel, T. W. Hänsch, and I. Bloch, Nature (London) **419**, 51 (2002).
[28] K. Pawłowski and K. Rzążewski, Phys. Rev. A **81**, 013620 (2010).
[29] A. Sinatra and Y. Castin, Eur. Phys. J. D **4**, 247 (1998).
[30] D. Witthaut, F. Trimborn, and S. Wimberger, Phys. Rev. Lett. **101**, 200402 (2008).
[31] D. Witthaut, F. Trimborn, and S. Wimberger, Phys. Rev. A **79**, 033621 (2009).
[32] A. Vardi and J. R. Anglin, Phys. Rev. Lett. **86**, 568 (2001).
[33] J. R. Anglin and A. Vardi, Phys. Rev. A **64**, 013605 (2001).
[34] D. Jaksch, C. Bruder, J. I. Cirac, C. W. Gardiner, and P. Zoller, Phys. Rev. Lett. **81**, 3108 (1998).
[35] R. Gati and M. K. Oberthaler, J. Phys. B **40**, R61 (2007).
[36] T. Gericke, P. Wurtz, D. Reitz, T. Langen, and H. Ott, Nat. Phys. **4**, 949 (2008).
[37] P. Würtz, T. Langen, T. Gericke, A. Koglbauer, and H. Ott, Phys. Rev. Lett. **103**, 080404 (2009).
[38] G. Barontini, R. Labouvie, F. Stubenrauch, A. Vogler, V. Guarrera, and H. Ott, Phys. Rev. Lett. **110**, 035302 (2013).
[39] D. Döring, G. R. Dennis, N. P. Robins, M. Jeppesen, C. Figl, J. J. Hope, and J. D. Close, Phys. Rev. A **79**, 063630 (2009).
[40] D. Schneble, G. K. Campbell, E. W. Streed, M. Boyd, D. E. Pritchard, and W. Ketterle, Phys. Rev. A **69**, 041601 (2004).
[41] Y. Yoshikawa, T. Sugiura, Y. Torii, and T. Kuga, Phys. Rev. A **69**, 041603 (2004).
[42] I. Tikhonenkov, J. R. Anglin, and A. Vardi, Phys. Rev. A **75**, 013613 (2007).
[43] K. Mølmer, Y. Castin, and J. Dalibard, J. Opt. Soc. Am. B **10**, 524 (1993).
[44] J. Johansson, P. Nation, and F. Nori, Comput. Phys. Commun. **184**, 1234 (2013).
[45] E. J. Mueller, T.-L. Ho, M. Ueda, and G. Baym, Phys. Rev. A **74**, 033612 (2006).
[46] R. Gati, J. Esteve, B. Hemmerling, T. B. Ottenstein, J. Appmeier, A. Weller, and M. K. Oberthaler, New J. Phys. **8**, 189 (2006).
[47] Y. Shin, M. Saba, T. A. Pasquini, W. Ketterle, D. E. Pritchard, and A. E. Leanhardt, Phys. Rev. Lett. **92**, 050405 (2004).
[48] Y. Castin and J. Dalibard, Phys. Rev. A **55**, 4330 (1997).
[49] C. N. Yang, Rev. Mod. Phys. **34**, 694 (1962).